ISSN 1749-3889 (print), 1749-3897 (online)
International Journal of Nonlinear Science
Vol.13(2012) No.2,pp.183-193

Numerical Solution for MHD Flow of Micro Polar Fluid Between Two Concentric Rotating Cylinders with Porous Lining

J V Ramana Murthy[1], G Nagaraju[2] *, K S Sai [3]
[1] Department of Mathematics, NIT Warangal, Warangal-506004, Andhra Pradesh, India.
[2]Department of Mathematics, GITAM University, Hyderabad campus,
Rudraram, Medak-502329, Andhra Pradesh, India.
[3] Department of Mathematics, DMSSVH College Of Engineering,
Machilipatnam, Krishna District, Andhra Pradesh, India
(Received 20 May 2011, accepted 30 November 2011)

Abstract: The steady flow of an electrically conducting, incompressible micropolar fluid in a narrow gap between two concentric rotating vertical cylinders with a thin porous lining under an external radial magnetic field is studied. Beavers and Joseph slip condition is taken at the porous lining boundary. The azimuthal velocity, micro-rotation component and slip velocity are evaluated. The effects of Hartmann number, the porous lining thickness parameter, the ratio of the angular velocities of the cylinders, the slip parameter, the porosity parameter, coupling number, couple stress parameters and Reynolds number on azimuthal velocity, micro-rotation velocity, slip velocity and coefficient of skin friction on cylinders are depicted through graphs.

Keywords: micropolar fluid; MHD flow; rotating cylinder; porous lining

1 Instroduction

The theory of micropolar fluids, as developed by Eringen [1, 2] has been a field of very active research for the last few decades as this class of fluids represent mathematically, many industrially important fluids such as paints, biological fluids, polymers, colloidal fluids, suspension fluids, etc. These fluids display the effects of local rotary inertia and couple stress and can be used to analyze the behavior of exotic lubricants, animal blood, etc. The study of micropolar fluid mechanics has received the attention of many researchers. A good list of references on the published papers for this fluid can be found in Eringen [3] and Hayakawa [4]. The Mathematical theory of equations of micropolar fluids and applications of these fluids in the theory of lubrication and in the theory of porous media is presented by Lukaszewicz [5]. However, the associated MHD problems have not received that much attention until recently.Flows through and past porous media with finite thickness are of relevance in many industrial applications like lubrication and tapping of solar energy. The control of shearing stress is important in the design of rotating machinery like totally enclosed fan cooled motors and lubrication industry in which centrifugal force plays a major role. Channabasappa et al [6] have examined the effect of porous lining thickness on velocity vector and shear stresses at the wall of inner and outer cylinders for the flow between two rotating cylinders. Sai [7] has studied the steady motion of an electrically conducting, incompressible viscous liquid in a narrow gap between two concentric rotating vertical cylinders in presence of an imposed magnetic field and he has presented the velocity profiles graphically. Bathaiah et al [8] have studied the viscous incompressible, slightly conducting fluid flow between two concentric rotating cylinders with non-erodable and non conducting porous lining on the inner wall of the outer cylinder under the influence of radial magnetic field of the form given in Hughes and Young and they have shown the effect of magnetic parameter, porous lining thickness, the ratio of the velocities of the cylinders, the slip parameter on velocity and temperature distributions graphically. Ramamurthy [9] have obtained the velocity distribution and magnetic field for a viscous incompressible conducting fluid between two coaxial rotating cylinders under the influence of radial magnetic field. Singh et al [10] have investigated the impulsive motion of a viscous liquid contained between two concentric circular cylinders in the presence of radial magnetic field. Sengupta et

*Corresponding author. *E-mail address*: naganitw@gmail.com Tel.: +91 9701274964.

IJNS.2012.04.15/592

al [11] studied the steady motion of an incompressible viscous conducting liquid between two porous concentric circular cylinders in presence of a radial magnetic field. Channabasappa et al [12] have studied the flow and heat transfer in an annulus between rotating cylinders. They have shown the effect of the thickness of the porous lining and the permeability on the velocity and Nusset number at the walls graphically. Subotic et al [13] have obtained the analytical solutions for the flow and temperature fields in an annulus with a porous sleeve between two rotating cylinders and they have presented in the form of graphs for the effects of Darcy number, Brinkman number and porous sleeve thickness on the velocity profile and temperature distribution. Channabasappa et al [14] have studied the stability analysis of laminar flow between two long concentric circular rotating cylinders with non-erodible porous lining on the outer wall of the inner cylinder and he has shown the effect of porous lining thickness on critical Taylor number graphically. Kamel [15] has studied the creeping motion of a polar fluid in the annular region between the two eccentric rotating cylinders. He depicted the dependence of the velocity components and the spin on the coupling number and the length ratio graphically. Meena et al [16] have studied the flow of a viscous incompressible fluid between two eccentric rotating porous cylinders with small suction/injection at both the cylinders and they have presented stream lines and pressure plots graphically. Borkakati et al [17] have examined the steady flow of an incompressible electrically conducting fluid between two coaxial cylinders in presence of radial magnetic field and they plotted graphically the heat transfer rate from the cylinders against the Hartmann number. Srinivasacharya et al [18] have studied the steady flow of incompressible and electrically conducting micropolar fluid flow between two concentric porous cylinders and they have presented the profiles of velocity and micro-rotation components for different micropolar fluid parameters and magnetic parameter.

In this paper, we study the steady incompressible electrically conducting micropolar fluid flow between two concentric rotating cylinders with porous lining in the presence of a radial magnetic field.

2 Formulation and solution of the problem

Consider the incompressible micropolar fluid flow between two concentric rotating cylinders of radii a and b $(a < b)$. The inner and outer cylinders are rotating with constant angular velocities Ω_1 and Ω_2 respectively. There is a non-erodible porous lining of thickness *h* on the inside of the outer cylinder. The flow is generated due to the rotation of these cylinders. The flow is subject to a magnetic field along the radial direction and no external electric field is applied. We assume that the induced magnetic field is much smaller than the externally applied magnetic field. Assume that the magnetic Reynolds number is very small, so that induced magnetic field and electric field produced by the motion of the electrically conducting fluid are negligible. The physical model of the problem is shown in Fig 1.

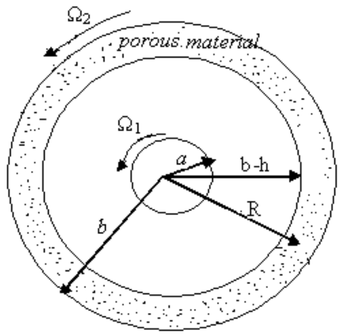

Fig 1. A section of the flow configuration

Choose the cylindrical polar coordinate system (R, θ, Z) with origin at the centre of the cylinder with Z axis along the axis of the cylinder and with (e_r, e_θ, e_z) as unit base vectors. Neglecting body forces and body couples, the field equations governing the micropolar fluid flow are

$$\nabla_1 \cdot \mathbf{Q} = 0 \tag{1}$$

$$\rho\mathbf{Q} \cdot \nabla_1\mathbf{Q} = -\nabla_1 \mathbf{P} + \kappa \nabla_1 \times \boldsymbol{l} - (\mu + \kappa) \nabla_1 \times \nabla_1 \times \mathbf{Q} + J \times B \tag{2}$$

$$\rho j\mathbf{Q} \cdot \nabla_1\boldsymbol{l} = -2\kappa\boldsymbol{l} + \kappa \nabla_1 \mathbf{Q} - \gamma \nabla_1 \times \nabla_1 \times \boldsymbol{l} + (\alpha + \beta + \gamma) \nabla_1 (\nabla_1 \cdot \boldsymbol{l}) \tag{3}$$

where $\mathbf{Q}$ is velocity vector, $\boldsymbol{l}$ is micro rotation vector, $\mathbf{P}$ is the fluid pressure, ρ and j are the fluid density and micro-gyration parameter,(μ, κ) and (α, β, γ) are viscosity and gyroviscosity coefficients. The current density *J*, magnetic field

B and electric field E are related by Maxwell's equations

$$\bigtriangledown_1 \times E = \frac{\partial B}{\partial t}, \bigtriangledown_1 \cdot B = 0, \bigtriangledown_1 \times B = \mu' J, \bigtriangledown_1 \cdot J = 0, J = \sigma_e \left(E + \mathbf{Q} \times B\right)$$

where $\bigtriangledown_1$ is the dimensional gradient, σ_e is electrical conductivity and μ' is the magnetic permeability. By nature of the flow, the velocity and micro-rotation components are axially symmetric and depend only on radial distance. Hence we assume that the velocity, micro-rotation vectors and the magnetic field are of the form

$$\mathbf{Q} = Ve_\theta, \boldsymbol{l} = \boldsymbol{C}e_z, B = \left(\frac{B_0}{R}\right) e_r \tag{4}$$

We introduce the following non-dimensional scheme

$$\left.\begin{array}{c} \mathbf{q} = \frac{\mathbf{Q}}{b\Omega_2}, r = \frac{R}{b}, \upsilon = \frac{\boldsymbol{l}}{\Omega_2}, p = \frac{\mathbf{P}}{\rho b^2 \Omega_2^2}, v = \frac{V}{b\Omega_2} \\ \boldsymbol{C} = \frac{C}{\Omega_2}, r_0 = \frac{a}{b}, \lambda = \frac{\Omega_1}{\Omega_2}, v_B = \frac{V_B}{b\Omega_2}, e = \frac{h}{b}, \sigma = \frac{b}{\sqrt{K}} \end{array}\right\} \tag{5}$$

where r_0 is ratio of radii, λ is the ratio of angular velocities, v_B is slip velocity, *e* is the porous lining thickness parameter and K is the porosity of the lining material. Using (5) in (2) and (3) we get the equations for the flow in the following non-dimensional form

$$Re\mathbf{q} \cdot \nabla \mathbf{q} = -Re\nabla p + c\nabla \times \upsilon - \nabla \times \nabla \times \mathbf{q} - \frac{M^2}{r^2}\mathbf{q} \tag{6}$$

$$\varepsilon \mathbf{q} \cdot \nabla \upsilon = -2s\upsilon + s\nabla \times \mathbf{q} - \nabla \times \nabla \times \upsilon + \frac{1}{\delta}\nabla(\nabla \cdot \upsilon) \tag{7}$$

where the non-dimensional parameters viz., Reynolds number Re, Hartmann number M, cross viscosity parameter or coupling number c, couple stress parameters s δ and gyration parameter ε are defined by

$$Re = \frac{\rho b^2 \Omega_2}{\mu + \kappa}, M = \sqrt{\frac{\sigma_e B_0^2}{\mu + \kappa}}, c = \frac{\kappa}{\mu + \kappa}, s = \frac{\kappa b^2}{\gamma}, \delta = \frac{\gamma}{\alpha + \beta + \gamma}, \varepsilon = \frac{\rho j b^2 \Omega_2}{\gamma} \tag{8}$$

The velocity and micro-rotation are now in the form

$$\mathbf{q} = v(r)e_\theta \quad and \quad \upsilon = C(r)e_z \tag{9}$$

Substituting (9) in (6) and comparing the components along e_r, e_θ directions, we get

$$\frac{dp}{dr} = \frac{v^2}{r} \tag{10}$$

$$-c\frac{dC}{dr} + D^2 v - \frac{M^2}{r^2} v = 0 \tag{11}$$

where $D^2 = \frac{d^2}{dr^2} + \frac{1}{r}\frac{d}{dr} - \frac{1}{r^2}$
Similarly using (9) in the equation (7), the axial direction component yields the following equation for micro-rotation C

$$-2sC + s\left(\frac{dv}{dr} + \frac{v}{r}\right) + \left(\frac{d^2 C}{dr^2} + \frac{1}{r}\frac{dC}{dr}\right) = 0 \tag{12}$$

Eliminating $\frac{dC}{dr}$ value from (11) and (12) we get the following equation for v

$$D^4 v - s\left(2 - c\right) D^2 v - M^2 D^2 \left(\frac{v}{r^2}\right) + 2sM^2 v = 0 \tag{13}$$

We note the following relations
$D^4 v = v^{iv} + \frac{2}{r}v''' - \frac{3}{r^2}v'' + \frac{3}{r^3}v' - \frac{3}{r^4}v$
$D^2(\frac{v}{r^2}) = \frac{1}{r^2}v'' - \frac{3}{r^3}v' + \frac{3}{r^4}v$
Using these two relations in (13) we get the equation for velocity v as

$$v^{iv} + \frac{2}{r}v''' + \left(a_1 + \frac{a_2}{r^2}\right) v'' + \left(\frac{a_1}{r} + \frac{a_3}{r^3}\right) v' + \left(\frac{a_4}{r^2} - \frac{a_3}{r^4}\right) v = 0 \tag{14}$$

where $a_1 = s(c-2), a_2 = -(3+M^2), a_3 = 3(1+M^2) \quad and \quad a_4 = s(2M^2c+2)$
Substituting $\frac{dC}{dr}$ value from equation (11) into (12) we get micro-rotation component C as

$$2scC = v''' + \frac{2}{r}v'' + \left(sc - \frac{a_3}{3r^2}\right)v' + \left(\frac{sc}{r} + \frac{a_3}{3r^3}\right) \tag{15}$$

The constants $a_1, a_2, a_3 \quad and \quad a_4$ can be found by using the no slip boundary condition on velocity V and hyper-stick boundary condition on micro-rotation $\boldsymbol{C}$. These conditions at the inner cylinder and at the porous lining of outer cylinder are explicitly given as below.

3 Boundary conditions

The equations (14) and (15) are solved for the velocities v and C and can be found by using the boundary conditions

$$\left.\begin{array}{c} V = a\Omega_1 \quad at \quad R = a \\ V = V_B \quad at \quad R = b-h \\ l_\Gamma = \frac{1}{2}\nabla \times \mathbf{Q}_\Gamma \quad at \quad R = a \\ l = 0 \quad at \quad R = b-h \end{array}\right\} \tag{16}$$

where Γ represents the boundary of inner cylinder and V_B is the slip velocity obtained by using Beavers and Joseph condition

$$\frac{dV}{dR} = \frac{\alpha}{\sqrt{K}}(V_B - Q_D) \quad at \quad R = b-h \tag{17}$$

Here α is the slip parameter and Q_D is the Darcy velocity in the porous lining.In equation (17), the Darcy's velocity Q_D is given by the relation

$$Q_D = R\Omega_2 + \Phi \tag{18}$$

where $\Phi = \frac{K}{\mu}\frac{\int_0^{2\pi}\int_{b-h}^{b}\rho R\Omega_2^2 R d\theta dR}{\int_0^{2\pi}\int_{b-h}^{b} R d\theta dR}$ which on simplification is given by

$$\Phi = \frac{2\rho K\Omega_2^2}{3\mu}\left(\frac{3b^2 - 3bh + h^2}{2b-h}\right) \tag{19}$$

The expression for Φ, as given above, is the one considered by channabasappa et al [6]. In relation (18), the two terms on RHS arise due to the rotation of the porous medium along with the outer cylinder. The four constants a_1, a_2, a_3 and a_4 can be found out numerically by using the above boundary conditions in (16)

4 Finite difference method of solution

In view of the complicated nature of two equations (14) and (15), the analytical solution seems to be beyond reach. Hence we use here Finite Difference Method for solution for v and C. We discretise the interval $[r_0, 1-e]$ into n subintervals with $n+1$ nodes, starting from first node r_0 to the last node $r_n = 1-e$. Each node is represented by $r_i = r_0 + ih$, with $h = \frac{1-e-r_0}{n}$ is the step length. The values of the functions v, C at r_i are given by v_i and C_i. The symmetric derivative formulae at the i'th node are given as below:

$$\left.\begin{array}{c} v_i^{'} = \frac{v_{i+1}-v_{i-1}}{2h} \\ v_i^{''} = \frac{v_{i+1}-2v_i+v_{i-1}}{h^2} \\ v_i^{'''} = \frac{v_{i+2}-2v_{i+1}+2v_{i-1}-v_{i-2}}{2h^2} \\ v_i^{iv} = \frac{v_{i+2}-4v_{i+1}+6v_i-4v_{i-1}+v_{i-2}}{h^4} \end{array}\right\} \tag{20}$$

Substituting these derivatives given in (29), in the equation (19) we get

$$t_{1,i}v_{i-2} + t_{2,i}v_{i-1} + t_{3,i}v_i + t_{4,i}v_{i+1} + t_{5,i}v_{i+2} = 0 \tag{21}$$

where

$$\left.\begin{array}{c} t_{1,i} = r_i^4 - hr_i^3 \\ t_{2,i} = -4r_i^4 + 2hr_i^3 + (a_1 r_i^2 + a_2) r_i^2 h^2 - (a_1 r_i^3 + a_3 r_i)\frac{h^3}{2} \\ t_{3,i} = 6r_i^4 - 2hr_i^2 (a_1 r_i^2 + a_2) + (a_4 r_i^2 - a_3) h^4 \\ t_{4,i} = -4r_i^4 - 2hr_i^3 + (a_1 r_i^2 + a_2) r_i^2 h^2 + (a_1 r_i^3 + a_3 r_i)\frac{h^3}{2} \\ t_{1,i} = r_i^4 + hr_i^3 \end{array}\right\} \tag{22}$$

we take the following boundary conditions

$$v_0 = v(r_0) = \lambda r_0 = n_1, \quad v_n = \frac{v_{n+1} - v_{n-1}}{2h\alpha\sigma} + n_2, \quad C_0 = \lambda, \quad and \quad C_n = 0 \tag{23}$$

where $n_2 = 1 - e + \frac{2Re(e^2 - 3e + 3)}{3\sigma^2(2-e)(1-c)}$ Evaluating (21) for different values of i we obtain

$$\left.\begin{array}{c} i = 0 : t_{1,0} v_{-2} + t_{2,0} v_{-1} + t_{4,0} v_1 + t_{5,0} v_2 = -t_{3,0} v_0 \\ i = 1 : t_{1,1} v_{-1} + t_{3,1} v_1 + t_{4,1} v_2 + t_{5,1} v_3 = -t_{2,1} v_0 \\ i = 2 : t_{2,2} v_1 + t_{3,2} v_2 + t_{4,2} v_3 + t_{5,2} v_4 = -t_{1,2} v_0 \\ . \\ . \\ . \\ i = n-1 : t_{1,n-1} v_{n-3} + t_{2,n-1} v_{n-2} + \left(t_{3,n-1} - \frac{t_{4,n-1}}{2h\alpha\sigma}\right) v_{n-1} + \left(t_{5,n-1} + \frac{t_{4,n-1}}{2h\alpha\sigma}\right) v_{n+1} = -t_{4,n-1} n_2 \\ i = n : t_{1,n} v_{n-2} + \left(t_{2,n} - \frac{t_{3,n}}{2h\alpha\sigma}\right) v_{n-1} + \left(t_{4,n} + \frac{t_{3,n}}{2h\alpha\sigma}\right) v_{n+1} + t_{5,n} v_{n+2} = -t_{3,n} n_2 \end{array}\right\} \tag{24}$$

The finite difference form of (15), will give us the equation

$$\begin{aligned} 2sch^3 r_i^3 C_i = -\frac{r_i^3}{2} v_{i-2} + \left(r_i^3 + 2hr_i^2 - \frac{h^2 r_i}{2}\left(r_i^2 sc - \frac{a_3}{3}\right)\right) v_{i-1} + \left(-4hr_i^2 + h^3 scr_i^2 + \frac{a_3 h^3}{3}\right) v_i \\ + \left(-r_i^3 + 2hr_i^2 + \frac{h^2 r_i}{2}\left(r_i^2 sc - \frac{a_3}{3}\right)\right) v_{i+1} + \frac{r_i^3}{2} v_{i+2} \end{aligned} \tag{25}$$

Using the boundary conditions $C_0 = \lambda$ and $C_n = 0$ in (25), we get

$$t_1 v_{-2} + t_2 v_{-1} + t_3 v_1 - t_1 v_2 = t_3 \quad and \quad t_5 v_{n-2} + t_6 v_{n-1} + t_7 v_{n+1} - t_5 v_{n+2} = t_8 n_2 \tag{26}$$

where
$t_1 = -\frac{r_0^3}{2}, \quad t_2 = r_0^3 + 2hr_0^2 - \frac{h^2 r_0}{2}\left(r_0^2 sc - \frac{a_3}{3}\right), \quad t_3 = -r_0^3 + 2hr_0^2 + \frac{h^2 r_0}{2}\left(r_0^2 sc - \frac{a_3}{3}\right)$
$t_4 = sch^3 r_0^2 + 4hr_0^2 - \frac{a_3 h^3}{3}, \quad t_5 = -\frac{r_n^3}{2}, \quad t_6 = r_n^3 + 2hr_n^2 - \frac{h^2 r_n}{2}\left(r_n^2 sc - \frac{a_3}{3}\right) - \frac{1}{2\alpha\sigma}\left(-4r_n^2 + h^2 scr_n^2 + \frac{a_3 h^2}{3}\right)$
$t_7 = -r_n^3 + 2hr_n^2 + \frac{h^2 r_n}{2}\left(r_n^2 sc - \frac{a_3}{3}\right) + \frac{1}{2\alpha\sigma}\left(-4r_n^2 + h^2 scr_n^2 + \frac{a_3 h^2}{3}\right), \quad t_8 = 4hr_n^2 - h^3 scr_n^2 - \frac{a_3 h^3}{3}$
Expressing the equations (24)-(26) in matrix form as follows:

$$AX = B \tag{27}$$

where

$$A = \left[\begin{array}{cccccccccccccc} t_1 & t_2 & t_3 & -t_1 & & & & & & & & & & \\ t_{1,0} & t_{2,0} & t_{4,0} & t_{5,0} & & & & & & & & & & \\ & t_{1,1} & t_{3,1} & t_{4,1} & t_{5,1} & & & & & & & & & \\ & & t_{2,2} & t_{3,2} & t_{4,2} & t_{5,2} & & & & & & & & \\ & & t_{1,3} & t_{2,3} & t_{3,3} & t_{4,3} & t_{5,3} & & & & & & & \\ & & & & & & & & & & & & & \\ & & & & & & & t_{1,n-3} & t_{2,n-3} & t_{3,n-3} & t_{4,n-3} & t_{5,n-3} & & \\ & & & & & & & & t_{1,n-2} & t_{2,n-2} & t_{3,n-2} & \left(t_{4,n-2} - \frac{t_{5,n-2}}{2h\alpha\sigma}\right) & \frac{t_{5,n-2}}{2h\alpha\sigma} & \\ & & & & & & & & & t_{1,n-1} & t_{2,n-1} & \left(t_{3,n-1} - \frac{t_{4,n-1}}{2h\alpha\sigma}\right) & \left(t_{5,n-1} + \frac{t_{4,n-1}}{2h\alpha\sigma}\right) & \\ & & & & & & & & & & t_{1,n} & \left(t_{2,n} - \frac{t_{3,n}}{2h\alpha\sigma}\right) & \left(t_{4,n} + \frac{t_{3,n}}{2h\alpha\sigma}\right) & t_{5,n} \\ & & & & & & & & & & t_5 & t_6 & t_7 & -t_5 \end{array}\right]$$

$X = [v_{-2}, v_{-1}, v_1, v_2, ..., v_{n-2}, v_{n-1}, v_{n+1}, v_{n+2}]^T$ and
$B = [t_4 v_0, -t_{3,0} v_0, -t_{2,1} v_0, -t_{1,2} v_0, 0, 0.., 0, -t_{5,n-2} n_2, -t_{4,n-1} n_2, -t_{3,n} n_2, t_8 n_2]^T$
where $v_0 = n_1$ is the value of v on the boundary and is known and solving the above system, we get the solution for v.

5 Skin friction

The constitutive equation for stress tensor T_{ij} of a micropolar fluid is given by

$$T_{ij} = (-P + \lambda \bigtriangledown \cdot \mathbf{Q})\delta_{ij} + (2\mu + \kappa)e_{ij} + \kappa\varepsilon_{ijm}(\omega_m - \boldsymbol{l}_m) \tag{28}$$

where ω_m is the vorticity vector, e_{ij} is strain rate tensor, δ_{ij} is Kronecker delta and ε_{ijm} is the alternating symbol.From equation (28), we get

$$\bar{T_{r\theta}} = \frac{dv}{dr} - (1-c)\frac{v}{r} - cC \tag{29}$$

where $\bar{T_{r\theta}} = \frac{T_{r\theta}}{\Omega_2(\mu+\kappa)}$ Hence the coefficient of skin friction on the inner and outer cylinders is given by

$$C_f = \frac{2T_{r\theta}}{\rho U^2} \quad at \quad R = a \quad and \quad R = b - h \tag{30}$$

where U=characteristic velocity=$b\Omega_2$, this can be written in the following non-dimensional form as

$$C_f = \frac{2\bar{T_{r\theta}}}{Re} \quad at \quad r = r_0 \quad and \quad r = 1 - e \tag{31}$$

6 Torque

The torque acting on the cylinders about the common axis of the cylinders is given by

$$\tau = (T_{r\theta} \times 2\pi R) \times R \tag{32}$$

Hence the non dimensional torque on inner and outer cylinders are given as

$$\bar{\tau_{in}} = 2\pi r_0^2 \quad \bar{T_{r\theta}} \mid_{r=r_0} \quad and \quad \bar{\tau_{out}} = 2\pi(1-e)^2 \quad \bar{T_{r\theta}} \mid_{r=1-e} \tag{33}$$

7 Results and discussions

The effects of the Hartmann number M, the porous lining thickness parameter e, the ratio of the angular velocities of the cylinders λ, the slip parameter α, the porosity parameter σ, Reynolds number Re, coupling number c and couple stress parameter s on azimuthal velocity v, micro-rotation velocity C, slip velocity v_B and the coefficient of skin friction at the inner and outer cylinders are numerically obtained and are depicted through Figs 2 to 28.

The azimuthal velocity v and micro-rotation velocity C, given in the equations (14) and (15), are computed for different values of M and e. Figs 2-7 show the azimuthal velocity v and micro-rotation velocity C against distance r for different values of M at a fixed value of porous lining thickness parameter $e = 0.1, 0.3, 0.4$. It is observed that v decreases and C increases as e increases. Again v decrease and C increase as M increases. It is observed that the nature of velocity profiles v is increasing with distance where as the micro-rotation C is increasing near to center of the cylinder and then C is decreasing as r increases. Figs 8 and 9 give the profiles of velocity v and micro-rotation C for different values of c. From (8) it is clear that an increase in coupling parameter c increases the values of the velocity v. Fig 9 shows that curves of micro-rotation component C with distance r are similar to parabolic path. It is interest that as coupling number c increases micro-rotation component C increases if c is more than 0.3. In Figs 10 and 11 the velocity profiles v and C plotted against Re. From this it is clear that an increase in Re increases both v and C. From Figs 12-13, it is seen that as the couple stress parameter s increases both v and C are increasing. But the effect of s on the values of v is not very significant. i.e., the variation in the values of s does not result in much variation in the values v. Figs 14-19 the velocity profiles are plotted against distance r for various values of the parameters e, α, σ. From these it is clear that both v and C decrease as e, α, σ increases. Fig 20 shows the slip velocity v_B against M for different values of e. We have observed that v_B increases with the increase in M. But it decreases with increase in e. In fig 21, v_B is plotted against e for different values of λ. We have noticed that the slip velocity exponentially decreases with increase in λ or e. Fig. 22 gives v_B plotted against σ for different values of α. we observe that v_B decreases with the increase in α or σ. The fall in the slip velocity, however, decreases with increase in α or σ. Figs 23-28 show the variation the coefficient of skin friction $C_f \mid_{in}$ and $C_f \mid_{out}$ at the inner and outer cylinders against c for different values of M, Re, s. We observe that skin friction C_f increases suddenly when c approaches 1. We observe that skin friction decreases with increasing values of Re, s whereas, the skin-friction $C_f \mid_{in}$ decreases with M and $C_f \mid_{out}$ at the outer cylinder increases with increasing values of M.

8 Conclusions

In this paper, the effect of radial magnetic field on micropolar fluid flow due to steady rotation of concentric cylinders with inner porous lining is examined. It is observed that as micro-polarity of the fluid effects the velocity but couple stress parameter can not effect the velocity profiles. As magnetic field strength increases velocity decreases and micro-rotation of the particles increases and there by skin friction decreases at inner cylinder and increases at outer cylinder.

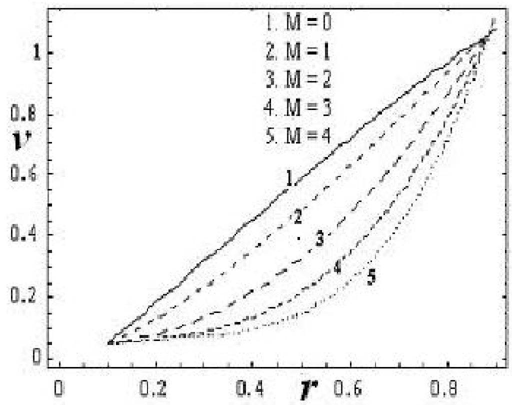

Fig 2 variation of v with M at $e = 0.1$

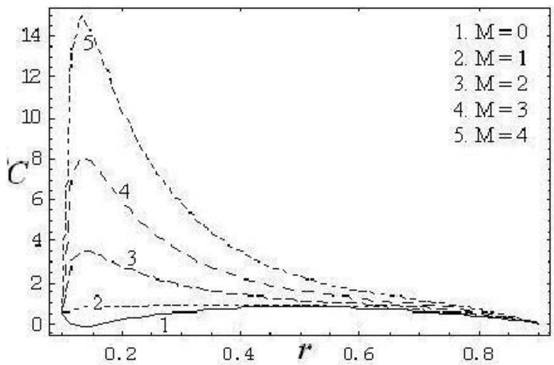

Fig 3 variation of C with M at $e = 0.1$

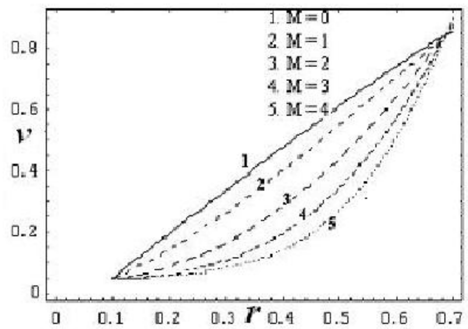

Fig 4 variation of v with M at $e = 0.3$

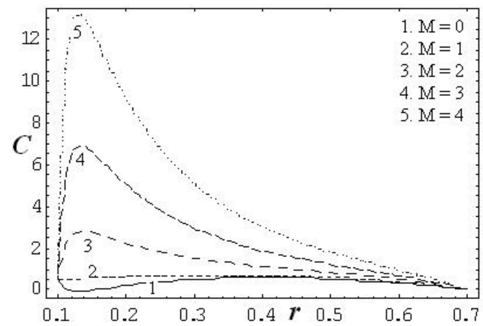

Fig 5 variation of C with M at $e = 0.3$

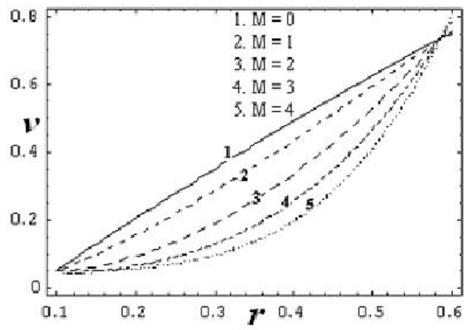

Fig 6 variation of v with M at $e = 0.4$

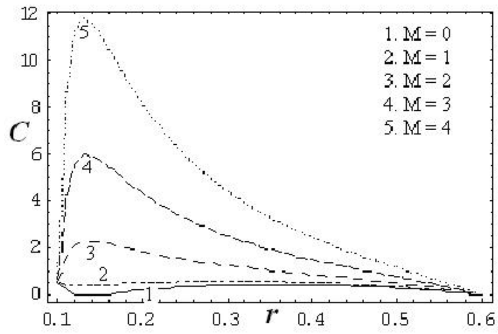

Fig 7 variation of C with M at $e = 0.4$

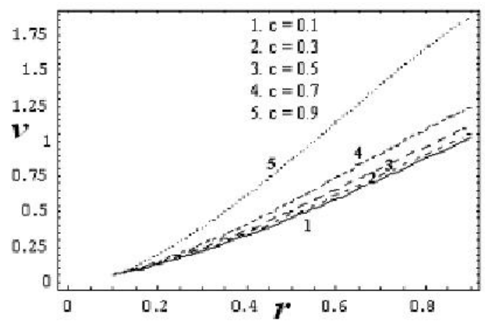

Fig 8 variation of v with c

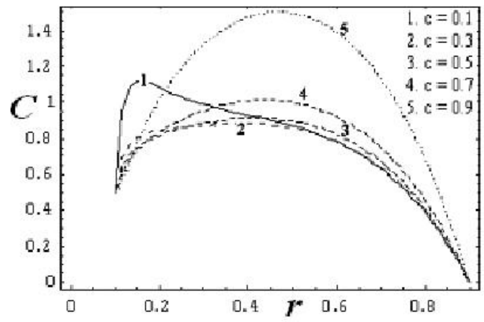

Fig 9 variation of C with c

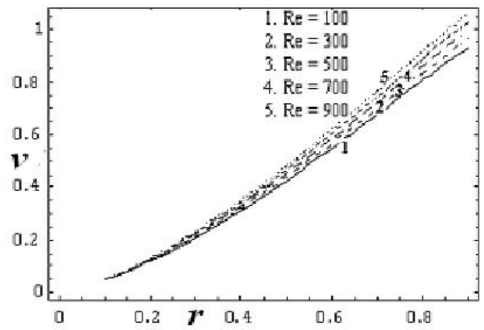

Fig 10 variation of v with Re

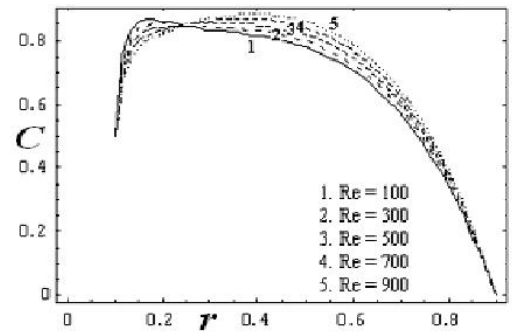

Fig 11 variation of C with Re

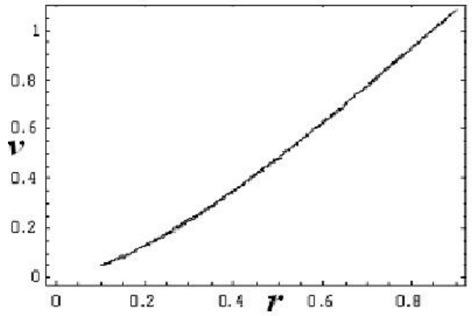

Fig 12 variation of v with s

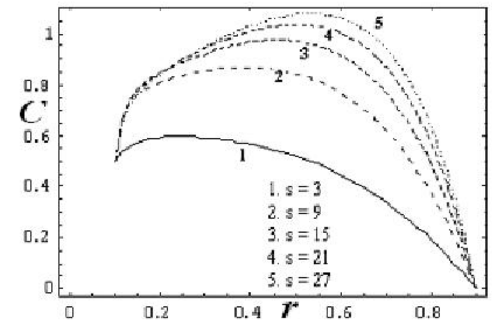

Fig 13 variation of C with s

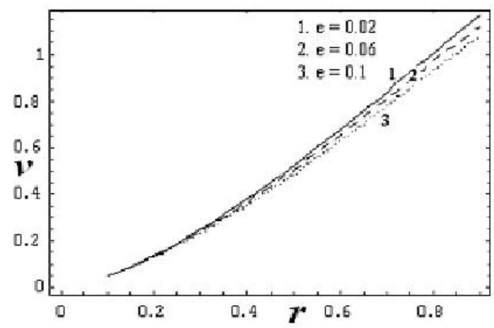

Fig 14 variation of v with e

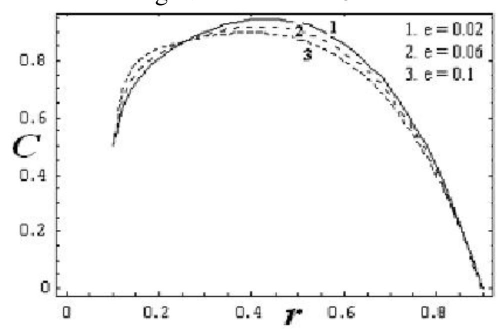

Fig 15 variation of C with e

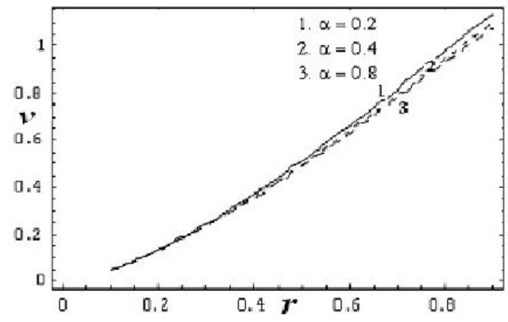

Fig 16 variation of v with α

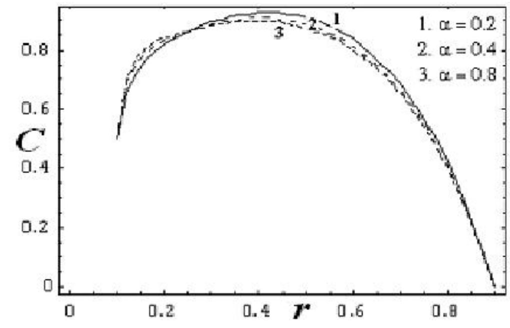

Fig 17 variation of C with α

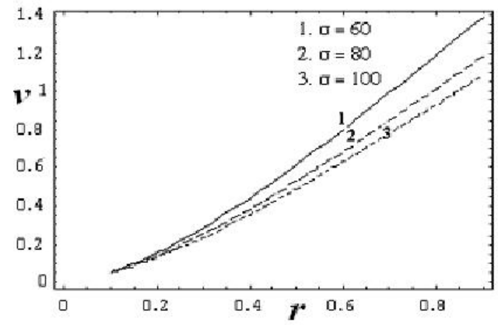

Fig 18 variation of v with σ

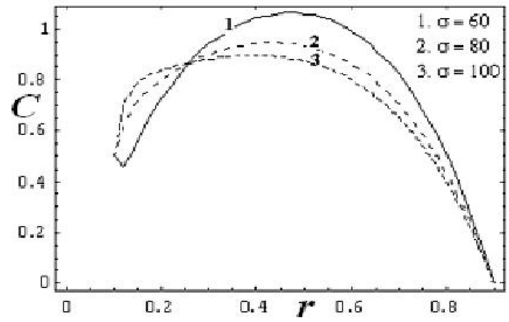

Fig 19 variation of C with σ

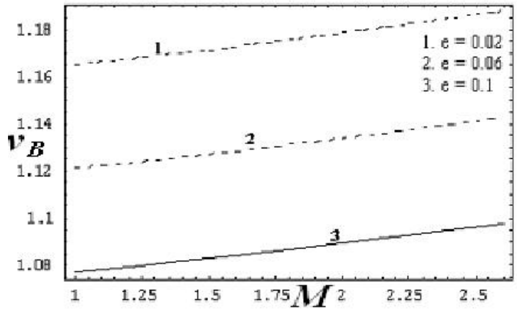

Fig 20 variation of v_B with e

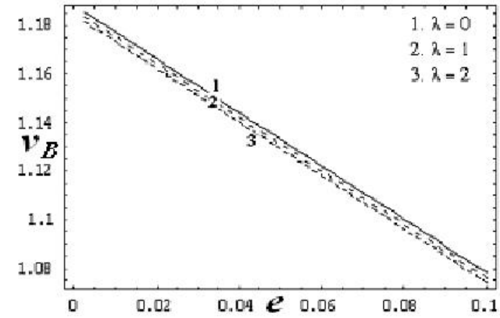

Fig 21 variation of v_B with λ

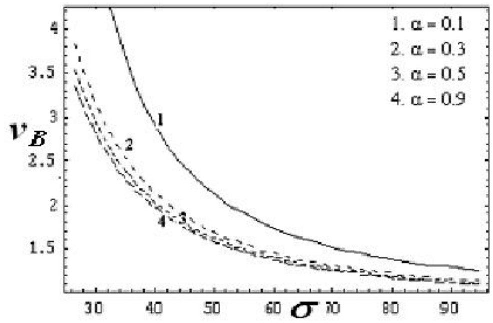

Fig 22 variation of v_B with α

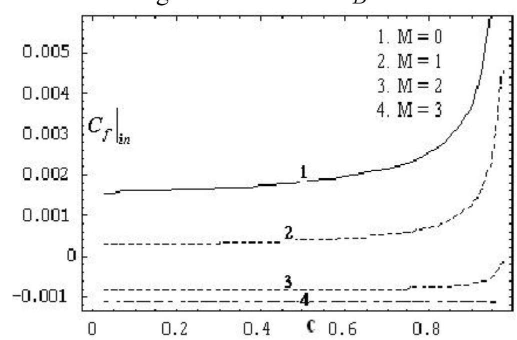

Fig 23 variation of $C_f \mid_{in}$ with M

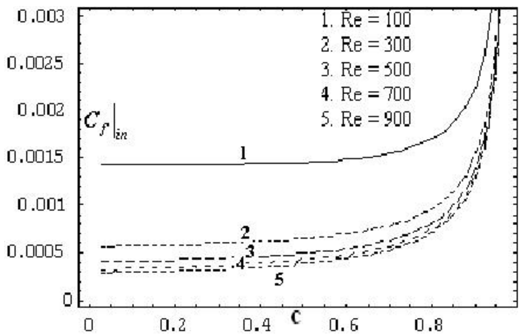

Fig 24 variation of $C_f \mid_{in}$ with Re

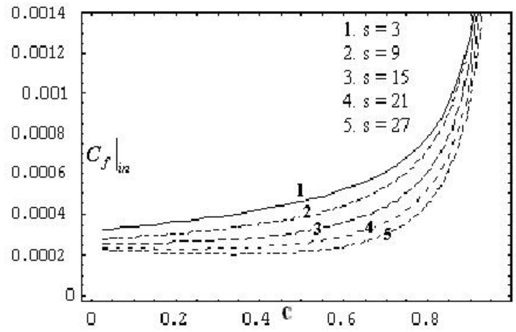

Fig 25 variation of $C_f \mid_{in}$ with s

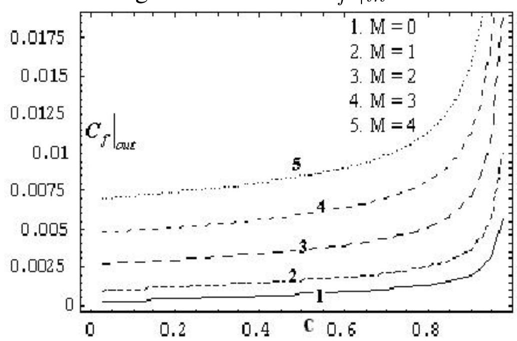

Fig 26 variation of $C_f \mid_{out}$ with M

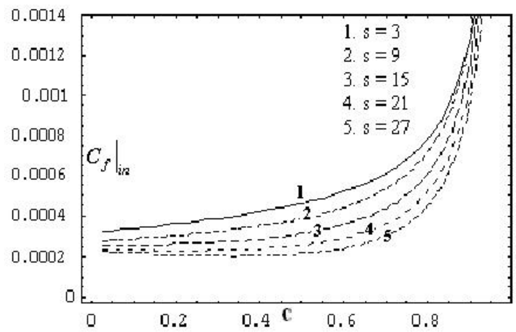

Fig 27 variation of $C_f \mid_{out}$ with Re

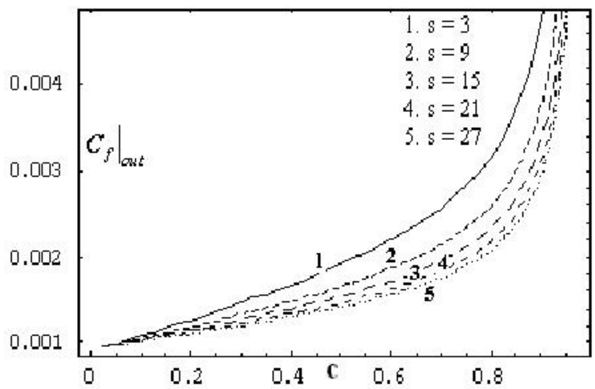

Fig 28 variation of $C_f \mid_{out}$ with s

References

[1] A C Eringen. Theory of micropolar fluids.*J. of Mathe.and Mech.*16(1966):1-18.
[2] A C Eringen.Theory of thermo micropolar fluids.*J. Math. Anal. Appl*.38(1972): 480-496.
[3] A C Eringen. Microcontinuum Field Theories II: Fluent Media, Springer, New York .(2001).
[4] H Hayakawa. Slow viscous flows in micropolar fluids. *Phy.Rev.E*.61(2000):5477-5492.
[5] G Lukaszewicz. "Micropolar fluids - theory and applications". Birkhauser, Boston (1999).
[6] M N Channabasappa, K G Umapathy and I V Nayak. Effect of porous lining on the flow between two concentric rotating cylinders. *Proc.Indian Acad.Sci*.88A(1979): 163-167.
[7] K S Sai. Mhd flow between two rotating cylinders with porous lining. *Rev.Roum.Phys*. 30(1985): 119-125.
[8] D Bathaiah and R Venugopal. Effect of porous lining on the Mhd flow between two concentric rotating cylinders under the influence of a radial magnetic field. *Acta. Mech*.44(1982): 41-158.

[9] P Ramamurthy. Flow between two concentric rotating cylinders with a radial magnetic field. *Phys.Fluids*.4(1961):1444.

[10] D Singh and Syed Ali Tahir Rizvi. Unsteady motion of a conducting liquid between two infinite coaxial cylinders.*Phys.Fluids*. 7(1964): 760-764.

[11] P R Sengupta and S K Ghosh. Hydromagnetic laminar flow of a conducting in an annulus in presence of a radial magnetic field. *Czech J. Phys*. 25(1975): 514-520.

[12] M N Channabasappa and K G Umapathy. Heat transfer by rotational flow in an annulus with porous lining. *Acta. Mech*. 23(1986): 243-248.

[13] M Subotic and F C Lai. Flows between rotating cylinders with a porous lining. *Journal of Heat Transfer*. 130(2008): 102601(1-6).

[14] M N Channabasappa, G Ranganna and B Rajappa. Stability of couette flow between rotating cylinders lined with porous material-I. *Indian J.Pure Appl.Math*. 14(1983): 741-756.

[15] M T Kamel. Flow of a polar fluid between two eccentric rotating cylinders, *Journal of Rheology*.29(1985): 37-48.

[16] S Meena, P Kandaswamy and Lokenath Debnath. Hydrodynamic flow between two eccentric cylinders with suction at the porous walls. *Int. J Math. Maths Sci*. 25(2001): 93-113.

[17] A K Borkakati and I Pop. Mhd Heat transfer in the flow between two coaxial cylinders. *Acta Mech*. 51(1984): 97-102.

[18] D Srinivasacharya and M Shiferaw. Numerical solution to the Mhd flow of micropolar fluid between two concentric porous cylinders. *Int. J. of Appl. Math. Mech*. 4(2008), 77-86.